Exploring the Pyroptosis-related Genes of Breast Cancer and their Effects on Tumor Immune Microenvironment

Congli Jia
Weifang Medical College
Fu Yang (dediracy1@163.com)
The First Affiliated Hospital of Kunming Medical University https://orcid.org/0000-0002-3298-6500
Ruining Li
Second Clinical Medical College of Lanzhou University

Research article

Keywords: breast cancer, genes, pyroptosis, tumor immune microenvironment

Posted Date: November 11th, 2021

DOI: https://doi.org/10.21203/rs.3.rs-1049643/v1

Abstract

Background: Breast cancer （BC） is the most common cancer among women, with high rates of metastasis and recurrence. Some studies have confirmed that pyroptosis is an immune-related programmed cell death. However, the correlation between the expression of pyroptosis-related genes in BC and its prognosis remains unclear.

Methods: In this study, we identified 38 pyroptosis-related genes that were differentially expressed between BC and normal tissues. The prognostic value of each pyroptosis-related gene was evaluated using patient data from The Cancer Genome Atlas (TCGA). The Cox regression method was performed to establish a prognostic model for 16-gene signature, classifying all BC patients in the TCGA database into a low-or high-risk group.

Results: The survival rate of BC patients in the high-risk group was significantly lower than that in the low-risk group (P0.01). Prognostic model is independent prognostic factor for BC patients compared to clinical features. Single sample gene set enrichment analysis (ssGSEA) showed a decrease for immune cells and immune function in the high-risk group.

Conclusions: Pyroptosis-related genes influence the tumor immune microenvironment and can predict the prognosis of BC.

Introduction

Breast cancer (BC) is the most common cancer among women aged 20 to 59, accounting for nearly a third of new cancers diagnosed in women [1]. It is a hereditary and multifactorial disease [2,3]. Worldwide, one million women are diagnosed with breast cancer, and about half of them die from the disease each year [4]. By 2020, approximately 26% of BC patients progressed to invasive BC, which may be associated with high mortality rate [5]. Despite advances in diagnosis and treatment, nearly 12% of breast cancer patients end up with metastasis or recurrence, with a poor prognosis [6]. At present, the main treatment of breast cancer remains surgery, combined with radiotherapy, chemotherapy and hormonal treatment when necessary. Immune treatment was also tried which has not benefited most patients, due to the high metastatic potential and lacking of comprehensive understanding for immune microenvironment of the tumor. Therefore, new therapeutic targets need to be discovered, and a new prognostic model that can assess patient risk and guide targeted therapy is urgently needed.

Pyroptosis is an inflammatory form of programmed cell death (PCD) characterized by cellular swelling and rupture, lysis, nuclear condensation, DNA fragmentation and IL-1β and IL-18 leakage [7], exacerbating the inflammatory response in the extracellular space [8]. It has been confirmed to be associated with inflammatory diseases and malignancies in humans. Gasdermins are a family of pore-forming proteins. It was found that the pore forming characteristics of n-terminal segments of Gasdermin D (GSDMD) and Gasdermin E (GSDME) were the driving factors of pyroptosis [9-11], these two kinds of proteins are cleaved by activated Caspase-1 and Caspase-3, respectively, leading to pyroptosis [9,12]. Further studies

showed that other members of the Gasdermin family, including GSDMA, GSDMB and GSDMC, also have membrane perforation ability and can activate pyroptosis [13]. Gasdermin protein family form pores of 10 ~ 20nm on the plasmolemma, subsequently cell contents, including IL-1β and IL-18, slowly leak from the pores, aggravating the inflammatory reaction in the intercellular space. Water molecules entering the cells lead to cell expansion, and rapid destruction of plasma membrane results in cell lysis characterized by nuclear condensation and DNA fragmentation of chromatin [14,15]. In previous studies, pyrophosis has been used primarily to fight infection by pathogens, which fight microbes by releasing damage-associated molecular patterns (DAMPs) that trigger inflammation [16-18]. Recent studies have shown that pyrophosis is closely related to antitumor immunity, which can trigger powerful antitumor immunity in vivo and in vitro, and immune checkpoint inhibitors (ICIs) can synergistically improve its efficacy [19,20]. Pyrophosis, though, is usually harmful to normal tissue [21], its exogenous activation induces powerful antitumor activity [22,23]. Cancers of the digestive [24,25], respiratory [26,27], reproductive [28,29] and hematopoietic [30,31] systems are sensitive to pyroptosis induction. Chemotherapeutic drugs, such as paclitaxel and cisplatin, effectively inhibit tumor proliferation and metastasis by inducing pyroptosis [32,33]. Zhang et al. showed that CD8+ T cells and NK cells induced pyroptosis of tumor cells through granase B (an enzyme that can lyse GSDME) in a pyroptosis activated microenvironment, thus establishing a positive feedback loop [34].

According to the existing reports, the role of pyroptosis in tumor development and anti-tumor process is undeniable. However, its role in BC is unclear. Therefore, we conducted a bioinformatics study to compare the expression level of pyroptosis-related genes in normal breast and BC tissues, construct a prognostic model according to the prognostic value of these genes, and study the effect of pyroptosis-related genes on tumor immune microenvironment.

Materials And Methods

Data preparation

The gene expression data of 1109 BC patients and 113 normal human breast tissue also with the corresponding clinical data were downloaded from TCGA database (https://portal.gdc.cancer.gov/repository).

Identification of differentially expressed pyroptosis-related genes

Based on 52 pyroptosis-related genes collected from previous literature, the R software was runned using the “limma” package to identify differentially expressed genes (DEGs) between tumor and normal samples with a P value <0.05. We established a PPI network for the DEGs by Search Tool for the Retrieval of Interacting Genes (STRING) (https://string-db.org/). A correlation graph for these DEGs was constructed applying R software.

Construction of prognostic model according to pyroptosis-related genes

To further explore the prognostic value of pyroptosis-related genes in breast cancer, Cox regression analysis was used to analyze the relationship between each gene and the patient's survival status, and screened 7 genes associated with prognosis. We then performed the multivariable Cox regression analysis to narrow down the candidate genes, ultimately a 5-gene signature prognostic model was constructed. The risk score for TCGA expression data was calculated using the “scale” function in R. BC patients in TCGA database were classified into high- or low-risk group based on the medium risk score, then we compared the overall survival (OS) time between two groups applying Kaplan–Meier analysis. PCA based on the 5-gene signature was performed by prcomp function of R. We employed the “survival”, “survminer” and “timeROC” R packages to develop the 1, 3 and 5- year ROC curve.

Independent prognostic analysis of the model

Clinical features including age, TNM stage and gender from TCGA database combined with risk score were analyzed employing Univariate and multivariable Cox regression analyses.

Functional enrichment analysis of the DEGs between the low- and high-risk groups

BC patients in the TCGA data were classified into two groups based on the median risk score. We screened out the DEGs between the low- and high-risk groups according to specific criteria (|log 2 FC| ≥1 and FDR<0.05). Gene ontology (GO) and Kyoto Encyclopedia of Genes and Genomes (KEGG) analyses based on these DEGs were performed using an online tool called the Database for Annotation Visualization and Integrated Discovery (DAVID)(http://david.abcc.ncifcrf.gov/).

Statistical analysis

We use Single-factor analysis of variance to compare the differences of gene expression between BC tissue and normal breast in TCGA database. The Pearson chi-square test was applied to compare the categorical variables. The OS of patients between high- and low-risk groups was compared employing Kaplan–Meier analysis. When evaluating the independent prognostic value of prognostic model, univariate and multivariate Cox regression was performed. The immune cell infiltration and immune pathway action between two groups were compared by the Mann–Whitney test. All statistical analyses were performed using R software (v4.1.1).

Results

Identification of DEGs between normal and BC tissues

The pyroptosis-related gene expression levels between 113 normal and 1109 BC tissues from TCGA database were compared, and 38 DEGs (P□0.01) were identified. Among them, 21 genes including NLRP7, GSDMC, AIM2, PYCARD, NOD2, NLRP6, IL18, BAX, GZMA, GSDMD, BAK1, CASP6, IRF1, CASP3, CYCS, CHMP4B, CHMP2A, CHMP4C, GSDMB, CHMP6, CASP8 were upregulated while 17 genes containing PLCG1, TIRAP, IRF2, GPX4, SCAF11, CHMP3, CASP4, CASP1, IL1B, NOD1, NLRP3, GSDME, PJVK, NLRP1, ELANE, TP63, IL6 were downregulated in the tumor group. The expression levels of these genes are shown in heatmap (Fig. 1A) (blue: low expression level; red: high expression level). We also created a protein–protein interaction (PPI) network diagram to show the interactions of these pyroptosis-related genes (Fig. 1B). The minimum required interaction score for the PPI analysis was set at 0.4 (the medium confidence). The number of edges in the network is 177 indicating that there are 177 interactions between these genes. The correlations network of all pyroptosis-related genes is shown in Fig. 1C (red: positive correlations; blue: negative correlations).

Tumor clustering based on DEGs

A consensus clustering analysis with all 1109 BC patients in the TCGA database was carried out, showing the relations between the expression of the 38 pyroptosis-related DEGs and BC subsets. We increased the clustering variable□K□from 2 to 10, and the results showed that when k=2, the intragroup correlations were the highest and intergroup correlations were low, suggesting that 1109 BC patients could be well divided into two groups according to 38 DEGs (Fig. 2A). The survival curve showed significant differences in OS between the two clusters (P□0.05) (Fig. 2B). Gene expression levels and clinical features including age (≤65 or□65 years), TNM and stages between the two clusters are shown on the heatmap (Fig. 2C), but no significant differences presented in clinical features between the two groups.

Identification of prognostic genes and construction of risk models based on TCGA database

We performed univariate Cox regression analysis on 1089 BC samples who have complete survival information in TCGA database, and 7 prognosis-related genes were identified. Among them, 6 genes (CHMP6, IL18, IRF1, IRF2, TP63, GZMA) were protective genes with HRs□1 while TIRAP□HR□1□was associated with high risk (Fig. 3A). By applying the Cox regression analysis, 5 characteristic genes (CHMP6, IL18, IRF2, TP63, TIRAP) were screened out to constructed prognostic model and the risk coef for each gene was calculated. 1089 BC patients were evenly assigned to the high- and low-risk groups based on the median risk score (Fig. 3B). The principal component analysis (PCA) demonstrated that patients could be well classified into high- or low-risk group (Fig. 3C). The survival chart showed that the number of deaths increased as the risk increased (Fig. 3D). We performed time-dependent receiver operating characteristic (ROC) analysis to evaluate the sensitivity and specificity of the prognostic model,

the result showed that the area under the ROC curve (AUC) was 0.707 for 1-year, 0.669 for 3-year, and 0.663 for 5-year survival (Fig. 3E). Significant difference in OS between the high and low risk groups was presented (P＜0.001)(Fig. 3F).

Independent prognostic value assessment of prognostic model

To evaluate whether the prognostic model based on gene signatures could be used as an independent prognostic factor, univariate and multivariable Cox regression analyses were applied. Both analyses demonstrated risk score as an independent prognostic factor (P＜0.01)（univariate：HR=1.926, 95% CI: 1.516–2.447; multivariable: HR=2.024, 95% CI: 1.553–2.639）(Fig. 4A and 4B). In addition, a heatmap showed the distribution of clinical features and signature genes in the high- and low-risk groups according to TCGA (Fig. 4C), in which we found that patient age and T stage distributed differently between the two groups (P＜0.01).

Functional enrichment analysis of prognostic models

By using R software, FDR＜0.05, $|\log_2 FC|$＞1 as screening conditions, we identified 19 DEGs between high- and low-risk groups. All the DEGs were downregulated in high-risk group. GO enrichment analysis and KEGG pathway analysis based on these DEGs were carried out, suggesting that the DEGs mainly enriched in immune response, chemokine-mediated signaling pathway, inflammatory response, cellular response to tumor necrosis factor, B cell receptor signaling pathway, positive regulation of B cell activation, Cytokine-cytokine receptor interaction and Chemokine signaling pathway (Fig. 5A and 5B).

Comparison of immune function between high and low risk groups

The single-sample gene set enrichment analysis (ssGSEA) was used to assess the immune cell infiltration and immune pathway action of each sample between the high - and low-risk groups in TCGA data. The distribution of immune cells showed that most immune cells were reduced in the high-risk group, especially $CD8^+$T cells, B cells, regulatory T (Treg) cells, T helper (Th) cells (Tfh, Th1, and Th2 cells) and natural killer (NK) cell (Fig. 6A). All immune pathways were reduced in the high-risk group (Fig. 6B).

Discussion

In this study, we first identified 38 differentially expressed pyroptosis-related genes between BC and normal tissue based on TCGA database. Significant differences in OS of two clusters classified according to 38 DEGs were presented, but not in clinical features. Subsequently, to further evaluate the prognostic value of these pyroptosis-related genes, a prognostic model based on 5 gene signatures was constructed,

applying the Cox regression analysis. The AUC of model for 1, 3 and 5 years were all greater than 0.6, indicating high accuracy of model predictions. Enrichment analysis suggested that DEGs between high- and low-risk group were closely related to immune function. Analysis of immune cell infiltration and immune function between the two groups showed that the infiltration of immune cells and the level of immune function were significantly reduced in the high-risk group.

Pyroptosis, an inflammatory - related programmed cell death, was demonstrated to affect the development and treatment of tumor from two aspects. On the one hand, the activation of pyroptosis results in the release of inflammatory mediators, such as IL-1 and IL-18, which might promote cancer development and progression [35,36]. some researchers even regard pyroptosis as another protumorigenic mechanism [37]. On the other hand, induction of pyroptosis has been shown to eradicate tumor cells from a variety of cancers [38]. In BC, whether pyroptosis-related genes affect the OS of patients and how to work on the tumor remain unclear. Our study built a prognostic model containing 5 pyroptosis-related characteristic genes (CHMP6, IL18, IRF2, TP63, TIRAP), which could access the risk and predict the prognosis of BC patients. Charged multivesicular body protein 6 (CHMP6) is a human ortholog of yeast vacuolar protein sorting (vps) 20, an acceptor for ESCRT-III on endosomal membranes and observed to regulate cargo sorting [39]. Fu et al. confirmed that CHMP6 induces oncosis, a form of cell death [40]. Oncosis is remarkable in ischemia, trauma and forms of neurodegeneration [41,42]. However, no relationship between CHMP6 and tumors has been found, and the mechanism by which it induces oncosis is not fully understood. In this study, CHMP6 is a pyroptosis-related gene that reduces the risk of BC survival, and we speculate that it may eradicate cancer cells by inducing oncosis and pyroptosis. Although the specific mechanism remains to be further studied, it is likely to be a regulatory factor and therapeutic target for BC. Interleukin 18 (IL-18) is a pleiotropic cytokine that produced by a variety of immune cells, but dendritic cells and macrophages are the primary sources of active IL-18 [43]. The main function of IL-18 is mediated through induction of interferon γ(IFN-γ) secretion from T helper (Th1) cells [44]. Studies have shown that IL18 has a dual effect on tumor cells which may due to the complexity of the human immune system [45]. On the one hand, some preclinical models proved that IL18 has antitumor activity [45]. It acts as a proinflammatory factor, recruiting immune cells to the tumor microenvironment to fight tumors, which matched our model that patients with increased immune cell infiltration in BC tissue have a reduced risk of survival. Existing evidence indicates that IL18 has a protective effect on colon cancer [46]. On the other hand, IL18 could promote metastasis by upregulating VEGF and CD44 [47]. However, whether the specific mechanism is just to induce pyroptosis of cancer cells needs further study. IRF2, a member of the IRF family,is a transcription factor [48]. Studies suggested that IRF2 positively regulated MHC-I pathway and negatively regulates PD-L1 expression [49]. The MHC-I pathway is essential for immune recognition and tumor elimination by CD8 + T cells. Progressing tumors are frequently associated with the MHC-1 deficiency [50] and downregulating the MHC-1 pathway is one way for cancers evading the immune system [51]. Another way cancer can avoid immune elimination is upregulating PD-L1, thus inhibiting Ag-specific CD8 + T cell function [52]. Therefore, IRF2 not only promotes pyroptosis, but also regulates immune microenvironment to fight tumors. Tumor protein 63 (TP63) is a member of the p53 family of transcription factors [53]. Previous

studies showed that tumor cells acquired super-enhancers by recruiting master transcription factors (TFs) to activate the oncogene expression [54,55]. TP63 was confirmed as master TFs of squamous cell carcinoma (SCC) [56,57], thus regulating super-enhancers to promote SCC growth. Interestingly, others have reported that loss of TP63 expression occurs in a large number of humans early and advanced cutaneous squamous cell carcinomas [58]. In addition, low expression of TP63 has also been found associated with shorter survival in other SCCs, which is consistent with our research that TP63 is a protective gene for BC. This phenomenon may be related to the fact that different subtypes of TP63 have different or even opposite functions on cells. To apply TP63 as a predictive target for BC, more research would be needed. Toll-Interleukin 1 Receptor (TIR) Domain Containing Adaptor Protein (TIRAP) is an important adaptor protein which belongs to the TLR/IL-1R superfamily [59], containing two domains, a phosphatidylinositol 4,5-bisphosphate (PIP2) binding domain (PBD) and a TIR domain. TIR Domain is mainly involved in a variety of protein-protein interactions associated with inflammation [60]. Our study also demonstrated that TIRAP is a cell inflammatory death-related gene in BC. It has been proved that the abnormal expression of TIRAP leads to a variety of tumors, such as lymphocytic leukemia [61] and gastric cancer [62]. Meanwhile, its expression is associated with a higher risk and lower survival of BC in our study. However, Whether and how TIRAP plays a role in the tumor immune microenvironment remains unclear.

So far, the research on pyroptosis is not comprehensive enough. Three of the five pyroptosis-related genes (IL18, IRF2, TIRAP) identified by our model could regulate inflammatory response, and we hypothesized that they affect the pyroptosis of BC cells through this way. Pyroptosis-related DEGs between the high- and low-risk groups in BC patients were analyzed for functional enrichment, and we found that they are mainly involved in immune response, chemotaxis of inflammatory cytokines and activation of inflammatory cells, indicating that pyroptosis could regulate the antitumor immunity of BC. Our study found that patients in the high-risk group of BC showed a decrease in immune cell infiltration and immune function activity, suggesting that impaired immune function in the high-risk group was associated with reduced anti-tumor ability. Interestingly, Treg cells have been reported to inhibit anti-tumor immunity and are associated with poor prognosis [63], while it reduced in high-risk group in our study, which may due to the different roles of its two subtypes. Therefore, it is necessary to identify the subtype of Treg cells in BC.

Conclusion

To sum up, pyroptosis-related genes are closely related to BC, due to its differentially expressed between BC and normal tissue. In addition, a prognostic model of BC according to 5 signature genes picked out based on TCGA database, and this model was proved to be an independent prognostic factor of BC. There were significant differences in immune cell infiltration and immune function activity between the high-and low-risk groups of the model, suggesting that pyroptosis-related genes have an effect on BC antitumor immunity. Our study provides novel predictive marker genes for the prognosis for BC and supplies new clues for immunotherapy of BC.

Abbreviations

BC: Breast cancer; TCGA: The Cancer Genome Atlas; ssGSEA: Single sample gene set enrichment analysis; PCD: programmed cell death; GSDMD: Gasdermin D; GSDME: Gasdermin E; GSDMA: Gasdermin A; GSDMB: Gasdermin B; GSDMC: Gasdermin C; DAMPs: damage-associated molecular patterns; ICIs: immune checkpoint inhibitors; DEGs: differentially expressed genes; STRING: Search Tool for the Retrieval of Interacting Genes; OS: overall survival; GO: Gene ontology; KEGG: Kyoto Encyclopedia of Genes and Genomes; DAVID: Database for Annotation Visualization and Integrated Discovery; PPI: protein–protein interaction; PCA: principal component analysis; ROC: receiver operating characteristic; AUC: area under the ROC curve.

Declarations

Funding:

No

Authors' contributions

Conceptualization, Congli Jia; Methodology, Congli Jia; Software, Congli Jia; Validation, Congli Jia; Formal Analysis, Congli Jia; Investigation, Fu Yang; Writing – Original Draft Preparation, Congli Jia; Writing – Review & Editing, Congli Jia; Visualization, Ruining Li; Supervision, Fu Yang; Project Administration, Fu Yang.

Consent for publication

All the authors agreed to publish the manuscript

Conflicts of Interest

The authors report no conflicts of interest in this work.

Acknowledgements

Thanks to TCGA database for the data.

Statement

The data in this paper came from TCGA public database, and the original data had passed the ethical review and obtained the written informed consent of the patients when provided. Our use of the data had passed the review of the Ethical Review Committee of Weifang Medical College again.

References

1. Waks AG & Winer EP; Breast Cancer Treatment: A Review. JAMA.2019; 321(3):288-300.
2. Lambert AW, Pattabiraman DR and Weinberg RA: Emerging biological principles of metastasis. Cell.2017; 168: 670-691.
3. Semenza GL: Molecular mechanisms mediating metastasis of hypoxic breast cancer cells. Trends Mol Med. 2012; 18: 534-543.
4. Jemal A, Bray F, Center MM, Ferlay J, Ward E and Forman D: Global cancer statistics. CA Cancer J Clin. 2011; 61: 69-90.
5. Coughlin SS and Ekwueme DU: Breast cancer as a global health concern. Cancer Epidemiol. 2009; 33: 315-318.
6. Bray F, Ferlay J, Soerjomataram I, Siegel RL, Torre LA, Jemal A. Global cancer statistics 2018: GLOBOCAN estimates of incidence and mortality worldwide for 36 cancers in 185 countries. CA Cancer J Clin. 2018; 68: 394–424.
7. Wallach D, Kang TB, Kovalenko A. Concepts of tissue injury and cell death in inflammation: a historical perspective. Nat Rev Immunol. 2014;14(1):51–9.
8. Kayagaki N, Stowe IB, Lee BL, O'Rourke K, Anderson K, Warming S, Cuellar T, Haley B, Roose-Girma M, Phung QT, Liu PS, Lill JR, Li H, Wu J, Kummerfeld S, Zhang J, Lee WP, Snipas SJ, Salvesen GS, Morris LX, Fitzgerald L, Zhang Y, Bertram EM, Goodnow CC, Dixit VM. Caspase-11 cleaves gasdermin D for non-canonical inflammasome signalling. Nature. 2015; 526(7575):666–71.
9. Shi JJ, Y. Zhao, K. Wang, XY. Shi, Y. Wang, HW. Huang, YH. Zhuang, T. Cai, FC. Wang,F. Shao, Cleavage of GSDMD by inflammatory caspases determines pyroptotic cell death,Nature. 2015; 526:660-665.
10. Kayagaki N, Stowe IB, Lee BL, O'Rourke K, Anderson K, Warming S, Cuellar T, Haley B, Roose-Girma M, Phung QT, Liu PS, Lill JR, Li H, Wu JS, Kummerfeld S, Zhang J, Lee WP, Snipas SJ, Salvesen GS, Morris LX, Fitzgerald L, Zhang YF, Bertram EM, Goodnow CC, Dixit VM. Caspase-11 cleaves gasdermin D for non-canonical inflammasome signaling. Nature. 2015; 526:666-671.
11. Ding JJ, Wang K, Liu W, She Y, Sun Q, Shi JJ, Sun HZ, Wang DC, Shao F. Pore-forming activity and structural autoinhibition of the gasdermin family. Nature. 2016; 535:111-116.
12. Wang YP, Gao WQ, Shi XY, Ding JJ, Liu W, He HB, Wang K, Shao F. Chemotherapy drugs induce pyroptosis through caspase-3 cleavage of a gasdermin. Nature. 2017; 547:99-103.
13. Wang Y, Gao W, Shi X, Ding J, Liu W, He H, Wang K, Shao F. Nature. 2017; 547: 99-103.

14. Zhang Y, Chen X, Gueydan C & Han J. Plasma membrane changes during programmed cell deaths. Cell Res. 2018; 28: 9–21.
15. Frank D & Vince J. Pyroptosis versus necroptosis: similarities, differences, and crosstalk. Cell Death Differ. 2019; 26: 99–114.
16. Duong BH, Onizawa M, Oses-Prieto JA, Advincula R, Burlingame A, Malynn BA, Ma A. A20 restricts ubiquitination of pro-interleukin-1β protein complexes and suppresses NLRP3 inflammasome activity. Immunity. 2015; 42:55–67.
17. Lawlor KE, Khan N, Mildenhall A, Gerlic M, Croker BA, D'Cruz AA, Hall C, Kaur Spall S, Anderton H, Masters SL, et al. RIPK3 promotes cell death and NLRP3 inflammasome activation in the absence of MLKL. Nat Commun. 2015; 6:6282.
18. Conos SA, Chen KW. Active MLKL triggers the NLRP3 inflammasome in a cell-intrinsic manner. Proc Natl Acad Sci U S A. 2017;114: E961–e969.
19. Socinski MA, Jotte RM, Cappuzzo F, Orlandi F, Stroyakovskiy D, Nogami N, Rodríguez-Abreu D, Moro-Sibilot D, Thomas CA, Barlesi F, et al. Atezolizumab for first-line treatment of metastatic nonsquamous NSCLC. N Engl J Med. 2018; 378:2288–301.
20. Antonia S, Goldberg SB, Balmanoukian A, Chaft JE, Sanborn RE, Gupta A, Narwal R, Steele K, Gu Y, Karakunnel JJ, Rizvi NA. Safety and antitumour activity of durvalumab plus tremelimumab in non-small cell lung cancer: a multicentre, phase 1b study. Lancet Oncol. 2016; 17:299–308.
21. Bergsbaken T, Fink SL, Cookson BT. Nat. Rev. Microbiol. 2009; 7: 99-109.
22. Wang YY, Liu XL, Zhao R. Induction of pyroptosis and its implications in cancer management. Front Oncol. 2019; 9:971.
23. Xia X, Wang X, Cheng Z, Qin W, Lei L, Jiang J, Hu J. The role of pyroptosis in cancer: pro-cancer or pro-“host”? Cell Death Dis. 2019; 10:650.
24. Wei Q, Zhu R, Zhu J, Zhao R, Li M. E2-induced activation of the NLRP3 inflammasome triggers pyroptosis and inhibits autophagy in HCC cells. Oncol Res. 2019; 27:827–34.
25. Qiu S, Liu J, Xing F. ‘Hints’ in the killer protein gasdermin D: unveiling the secrets of gasdermins driving cell death. Cell Death Differ. 2017; 24:588–96.
26. Xi G, Gao J, Wan B, Zhan P, Xu W, Lv T, Song Y. GSDMD is required for effector CD8(+) T cell responses to lung cancer cells. Int Immunopharmacol. 2019; 74:105713.
27. Lu H, Zhang S, Wu J, Chen M, Cai MC, Fu Y, Li W, Wang J, Zhao X, Yu Z, et al. Molecular targeted therapies elicit concurrent apoptotic and GSDME-dependent pyroptotic tumor cell death. Clin Cancer Res. 2018; 24:6066–77.
28. Hoseini Z, Sepahvand F, Rashidi B, Sahebkar A, Masoudifar A, Mirzaei H. NLRP3 inflammasome: Its regulation and involvement in atherosclerosis. J Cell Physiol. 2018; 233:2116–32.
29. So D, Shin HW. Cervical cancer is addicted to SIRT1 disarming the AIM2 antiviral defense. Oncogene. 2018; 37:5191–204.

30. Okondo MC, Johnson DC, Sridharan R, Go EB, Chui AJ, Wang MS, Poplawski SE, Wu W, Liu Y, Lai JH, et al. DPP8 and DPP9 inhibition induces procaspase-1-dependent monocyte and macrophage pyroptosis. Nat Chem Biol. 2017; 13:46–53.
31. Johnson DC, Taabazuing CY, Okondo MC, Chui AJ, Rao SD, Brown FC, Reed C, Peguero E, de Stanchina E, Kentsis A. DPP8/DPP9 inhibitor-induced pyroptosis for treatment of acute myeloid leukemia. Nat Med. 2018; 24:1151–6.
32. Zhang CC, Li CG, Wang YF, Xu LH, He XH, Zeng QZ, Zeng CY, Mai FY, Hu B, Ouyang DY. Chemotherapeutic paclitaxel and cisplatin differentially induce pyroptosis in A549 lung cancer cells via caspase-3/GSDME activation. Apoptosis. 2019; 24:312–25.
33. Wang F, Liu W, Ning J, Wang J, Lang Y, Jin X, Zhu K, Wang X, Li X, Yang F, et al. Simvastatin suppresses proliferation and migration in non-small cell lung cancer via pyroptosis. Int J Biol Sci. 2018; 14:406–17.
34. Zhang Z, Zhang Y, Xia S, Kong Q, Li S, Liu X, Junqueira C, Meza-Sosa KF, Mok TMY, Ansara J, et al. Gasdermin E suppresses tumour growth by activating anti-tumour immunity. Nature. 2020; 579:415–20.
35. Hu B, Elinav E, Huber S, Booth CJ, Strowig T, Jin C, Eisenbarth SC, Flavell RA. Inflammation-induced tumorigenesis in the colon is regulated by caspase-1 and NLRC4. Proc Natl Acad Sci U S A. 2010; 107:21635–40.
36. Janowski AM, Kolb R, Zhang W, Sutterwala FS. Beneficial and detrimental roles of NLRs in carcinogenesis. Front Immunol. 2013; 4:370.
37. Dunn JH, Ellis LZ, Fujita M. Inflammasomes as molecular mediators of inflammation and cancer: potential role in melanoma. Cancer Lett. 2012; 314:24–33.
38. Yu J, Li S, Qi J, Chen Z, Wu Y, Guo J, Wang K, Sun X, Zheng J. Cleavage of GSDME by caspase-3 determines lobaplatin-induced pyroptosis in colon cancer cells. Cell Death Dis. 2019; 10:193.
39. Yorikawa C, Shibata H, Waguri S, Hatta K, Horii M, Katoh K, Kobayashi T, Uchiyama Y and Maki M. Human CHMP6, a myristoylated ESCRT-III protein, interacts directly with an ESCRT-II component EAP20 and regulates endosomal cargo sorting. Biochem J. 2005; 387: 17-26.
40. Dongxu F, Linjie T, Zhi P, Weiwei D, Jinsong Y, Dalong M, Taiping S, Dianjun L and Ying W. Overexpression of CHMP6 induces cellular oncosis and apoptosis in HeLa cells. Biosci. Biotechnol. Biochem. 2009; 73 (3): 494-501.
41. Zong WX and Thompson CB. Necrotic death as a cell fate. Genes Dev. 2006; 20: 1-15.
42. Yuan J. Divergence from a dedicated cellular suicide mechanism: exploring the evolution of cell death. Mol. Cell. 2006; 23: 1-12.
43. Dinarello CA. Interleukin 1 and interleukin 18 as mediators of Inflammation and the aging process. Am J ClinNutr. 2006; 83: 447S.
44. Okamura H, Nagata K, Komatsu T, et al. A novel costimulatory factor for gamma interferon induction found in the livers of mice causes endotoxic shock. Infect Immun. 1995; 63: 3966.

45. Fabbi M, Carbotti G, Ferrini S. Context-dependent role of IL-18 in cancerbiology and counter-regulation by IL-18BP. J LeukocBiol 2015; 97:665-675.
46. Pagès F, Berger A, Henglein B, et al. Modulation of interleukin-18 expression in human coloncarcinoma: consequences for tumor immune surveillance. Int J Cancer. 1999; 84:326.
47. Palma G, Barbieri A, Bimonte S, et al. Interleukin 18: friend or foe in cancer. Biochim Biophys Acta 2013; 1836:296.
48. Karki R, Lee E, Place D, Samir P, Mavuluri J, Sharma B R, Balakrishnan A, R. Malireddi R K S, Geiger R, Zhu Q, Neale G, Kanneganti T D. IRF8 Regulates Transcription of Naips for NLRC4 Inflammasome Activation. Cell.2018; 173: 920–9333.e13.
49. Kaplan, DH, Shankaran V, Dighe AS, Stockert E, Aguet M, Old LJ and Schreiber RD. Demonstration of an interferon gamma-dependent tumor surveillance system in immunocompetent mice. Proc. Natl. Acad. Sci. USA.1998; 95:7556–7561.
50. Marincola FM, Jaffee EM, Hicklin DJ and Ferrone S. Escape of human solid tumors from T-cell recognition: molecular mechanisms and functional significance. Adv. Immunol. 2000; 74: 181–273
51. Shankaran V, Ikeda H, Bruce A T, White J M, Swanson P E, Old L J and Schreiber R D. IFN gamma and lymphocytes prevent primary tumour development and shape tumour immunogenicity. Nature.2001; 410: 1107–1111.
52. Yu H, Boyle TA, Zhou C, Rimm DL and Hirsch FR. PD-L1 expression in lung cancer. J. Thorac. Oncol. 2017; 12: 157–159.
53. Soares E. and Zhou H. Master regulatory role of p63 in epidermal development and disease. Cell. Mol. Life Sci.2018; 75, 1179-1190.
54. Hah, N. et al. Inflammation-sensitive super enhancers form domains of coordinately regulated enhancer RNAs. Proc. Natl Acad. Sci. USA. 2015; 112: E297–E302.
55. Pefanis E. et al. RNA exosome-regulated long non-coding RNA transcription controls super-enhancer activity. Cell. 2015; 161: 774–789.
56. Jiang YY. et al. Targeting super-enhancer-associated oncogenes in oesophageal squamous cell carcinoma. Gut. 2017; 66: 1358–1368.
57. Saladi S. V. et al. ACTL6A is co-amplified with p63 in squamous cell carcinoma to drive YAP activation, regenerative proliferation, and poor prognosis. Cancer Cell. 2017; 31: 35–49.
58. Lakshmanachetty S,Balaiya V, Johnson L K, Koster M L. TRP63/TP63 loss accelerates skin tumorigenesis through activation of Wnt/β-catenin signaling. Journal of Dermatological Science. 2018.
59. Narayanan KB, Park HH. Toll/interleukin-1 receptor (TIR) domain-mediated cellular signaling pathways. Apoptosis. 2015; 20: 196–209.
60. Bernard NJ, O'Neill LA. Mal, More Than a Bridge to Myd88. IUBMB Life. 2013; 65(9):777–86.
61. Antosz H, Sajewicz J, Marzec-Kotarska B, Dmoszynska A, Baszak J, Jargiello-Baszak M. Aberrant TIRAP and MyD88 expression in B-cell chronic lymphocytic leukemia. Blood Cells Mol. Dis. 2013; 51:

48–55.

62. Kennedy CL, Najdovska M, Tye H, McLeod L, Yu L, Jarnicki A, Bhathal PS, Putoczki T, Ernst M, Jenkins BJ. Differential role of MyD88 and Mal/TIRAP in TLR2-mediated gastric tumourigenesis. Oncogene. 2014; 33: 2540–2546.

63. Toker A. et al. Regulatory T cells in ovarian cancer are characterized by a highly activated phenotype distinct from that in melanoma. Clin. Cancer Res. 2018; 24: 5685–5696.

Figures

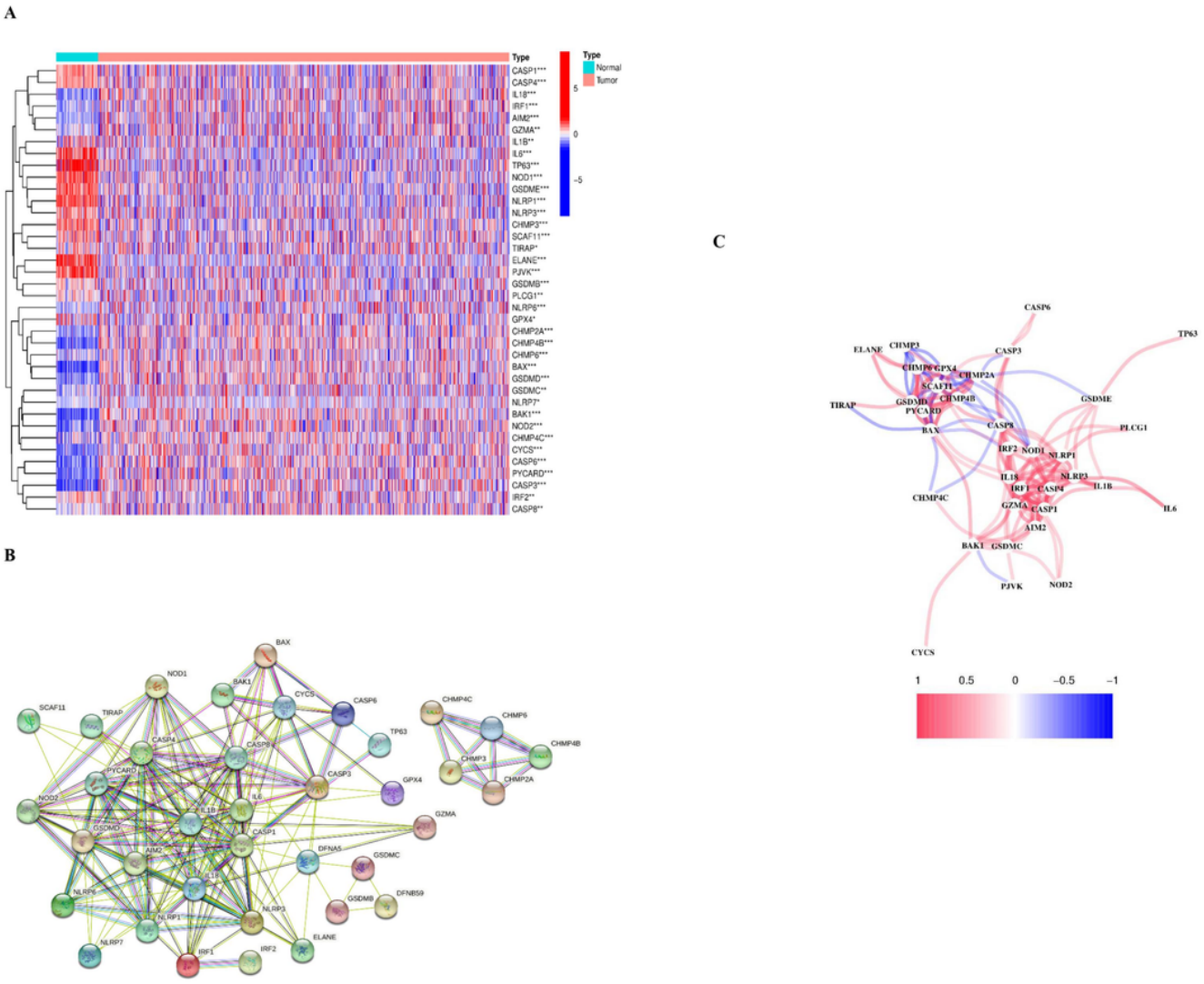

Figure 1

Expressions of the 38 pyroptosis-related genes and the interactions among them. A Heatmap (blue: low expression level; red: high expression level) of the pyroptosis-related genes between the normal (brilliant blue) and the tumor tissues (red). P values were showed as: **P<0.01; ***P<0.001. B PPI network showing

the interactions of the pyroptosis-related genes (interaction score=0.4). C The correlation network of the pyroptosis-related genes (red line: positive correlation; blue line: negative correlation. The depth of the colours reflects the strength of the relevance).

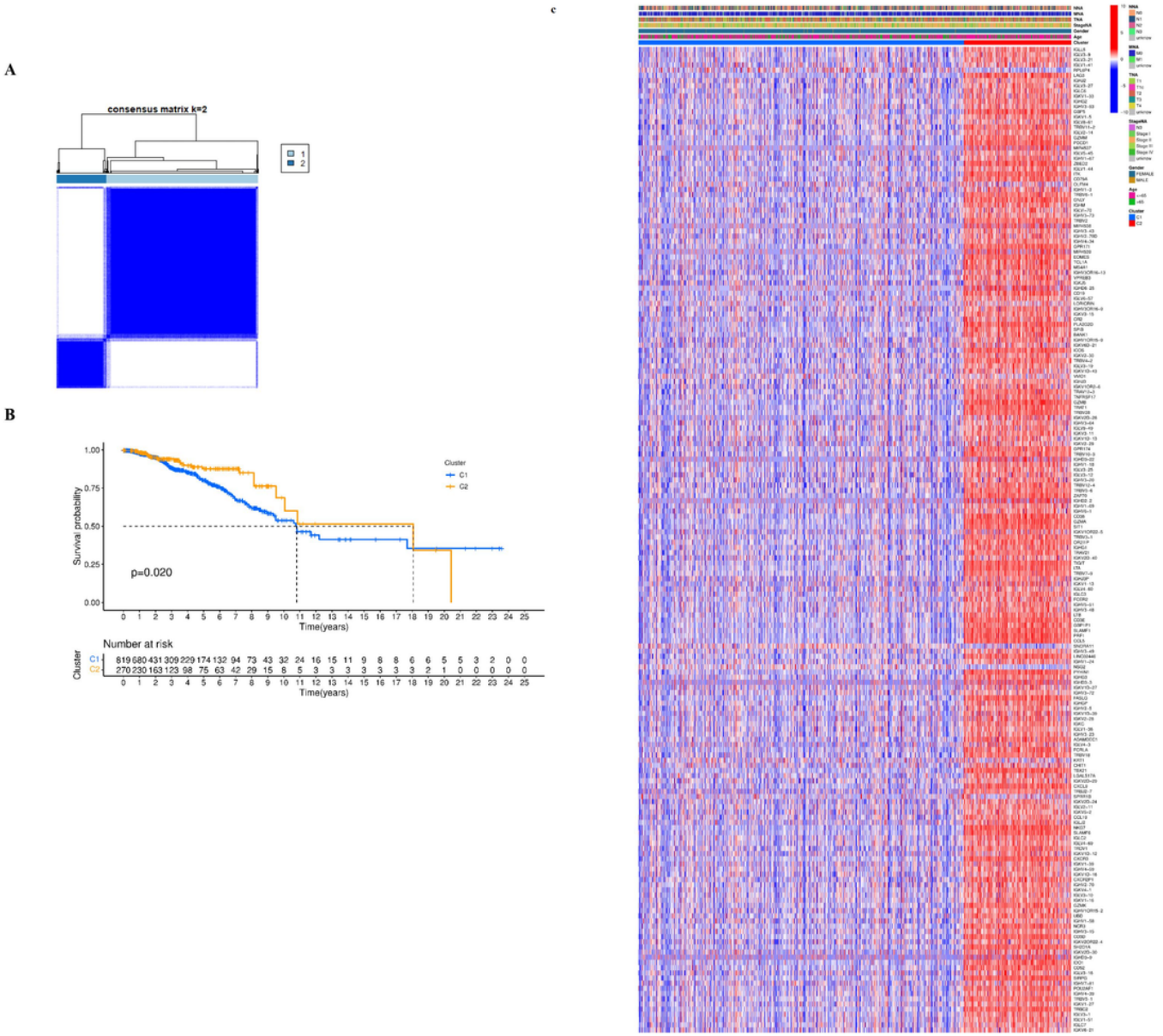

Figure 2

Tumor classification based on the pyroptosis-related DEGs. A 1109 BC patients were classified into two clusters according to the consensus clustering matrix (k=2). B Kaplan–Meier OS curves for the two clusters. C Heatmap of gene expression levels and clinical features for the two clusters classified by these DEGs (TNM is tumor stage. T: Tumor; N: Lymph Node; M: Metastasis).

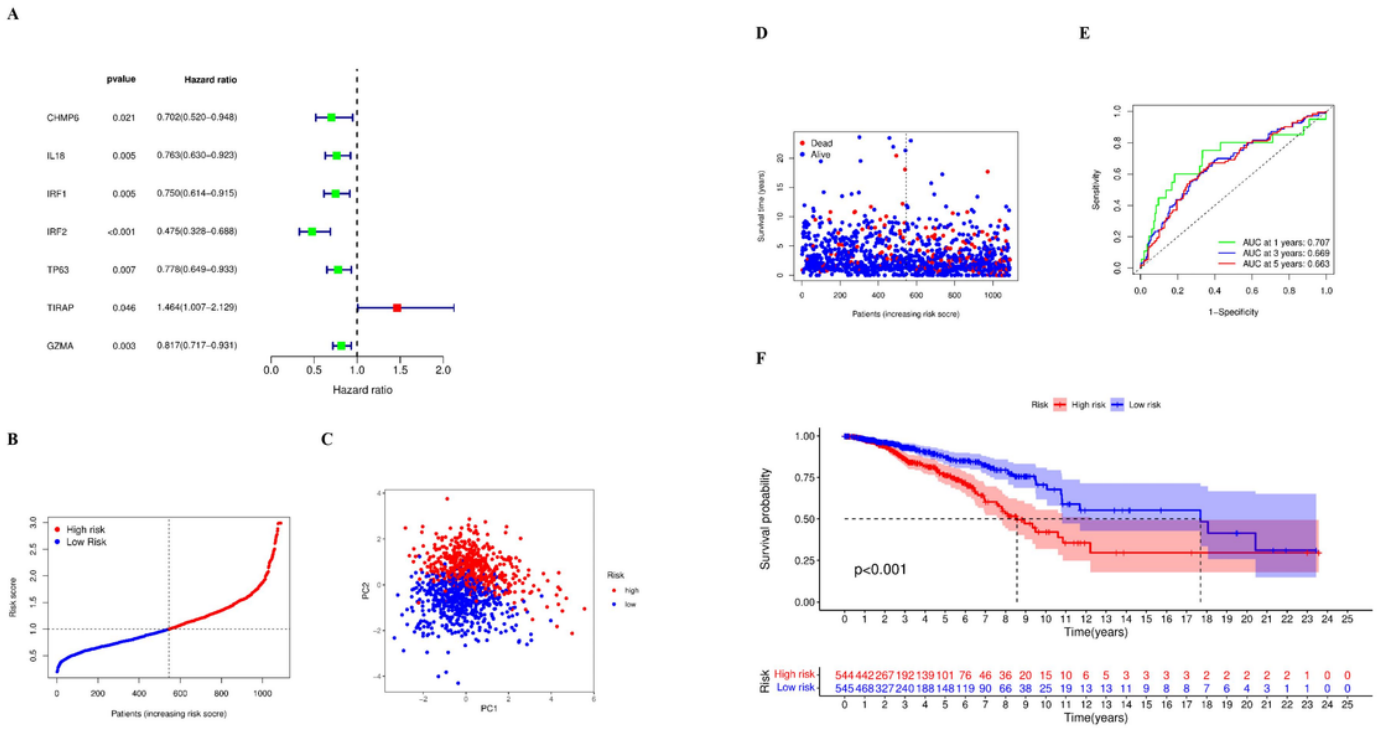

Figure 3

Construction of risk model based on the TCGA database. A Univariate cox regression analysis of OS for each pyroptosis-related gene, and 7 genes with P <0.05. B Distribution of patients based on the risk model. C PCA plot for BC patients based on the risk model. D The survival status for each patient (low-risk samples: on the left side of the dotted line; high-risk samples: on the right side of the dotted line). E ROC curves suggested the predictive accuracy of the risk model. F Kaplan–Meier curves for the OS of patients in the high- and low-risk groups.

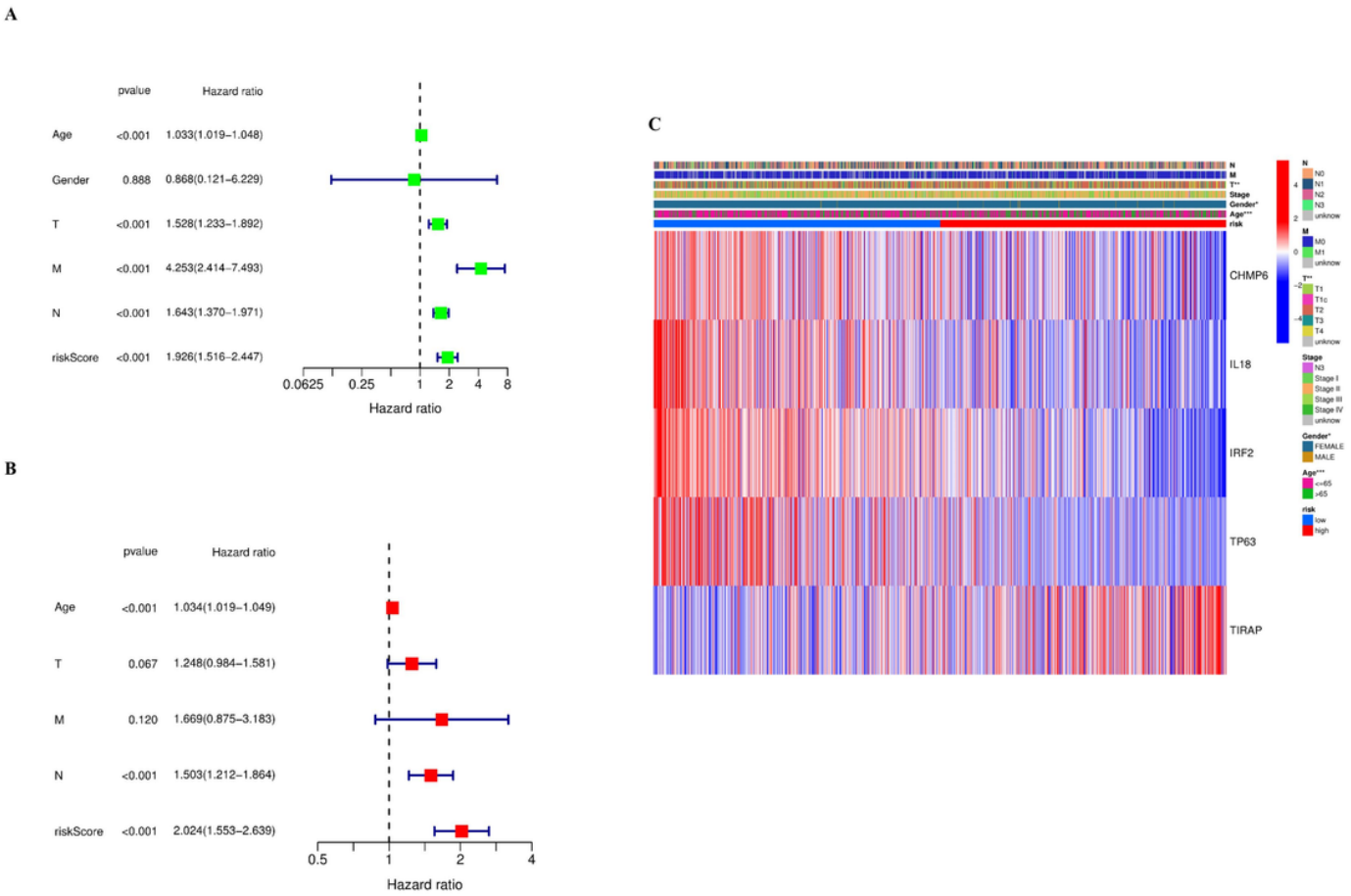

Figure 4

Univariate and multivariate Cox regression analyses for the risk model. A Univariate analysis for the TCGA samples (TNM is tumor stage. T: Tumor; N: Lymph Node; M: Metastasis). B Multivariate analysis for the TCGA samples. C heatmap showed the distribution of clinical features and signature genes in the high and low risk groups.

A

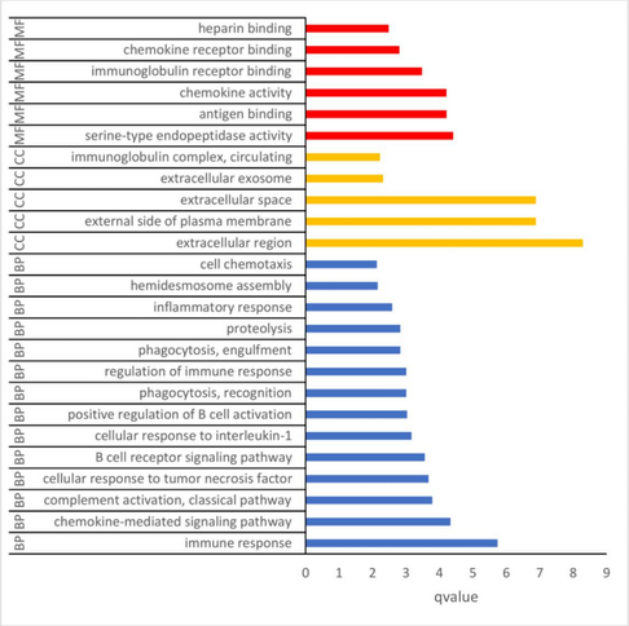

B

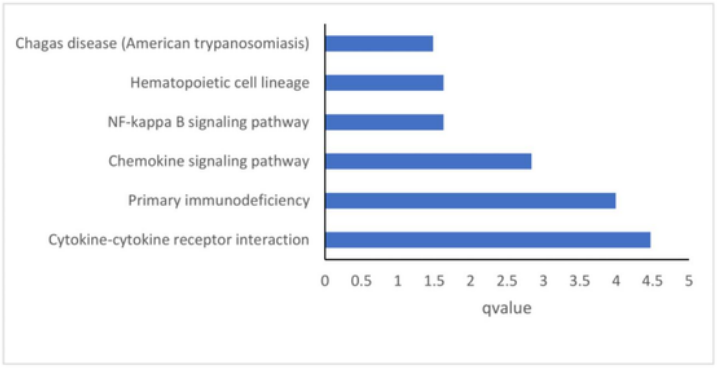

Figure 5

Functional enrichment analysis based on the DEGs between the two-risk groups for the TCGA samples. A GO enrichment (BP: Biological process; CC: Cellular component; MF: Molecular function). B KEGG enrichment.

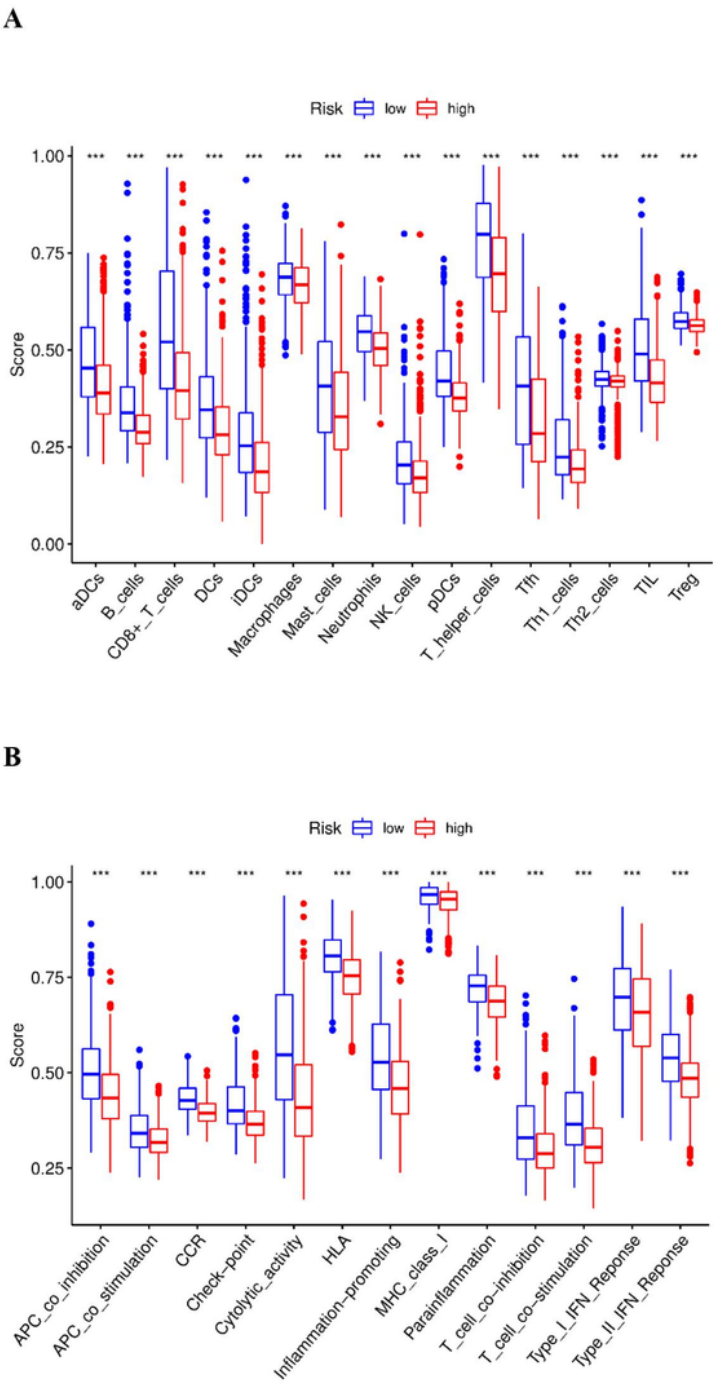

Figure 6

Comparison of the ssGSEA scores for immune cells and immune pathways. A Comparison of the infiltration degree for 16 types of immune cells. B Comparison of the activity for 13 types of immune pathways.